JSEE Vol. 24, No. 3&4, 2022 DOI: 10.48303/jsee.2023.1999909.1058

Research Paper

Determination of the Fault Plane of the 2017 Iranian Sefidsang Earthquake, Mw 6.0, by Seismic Moment Tensor Inversion Method

Ali Songhori[1], Mehrdad Pakzad[2*], Ahmad Sadidkhouy[2] and Zahra Khorrami[1]

1. Ph.D. Candidate, Seismology Department, Institute of Geophysics, University of Tehran, Tehran, Iran
2. Assistant Professor, Seismology Department, Institute of Geophysics, University of Tehran, Tehran, Iran,

*Corresponding Author; email: pakzad@ut.ac.ir

Received: 25/04/2023
Revised: 07/08/2023
Accepted: 02/09/2023

ABSTRACT

Essentially, assuming a simple fault model, the hypocenter and centroid should be located on the same plane. This approximation can help to distinguish the fault plane from the auxiliary plane of an earthquake in many situations. On April 5, 2017, the Sefidsang earthquake Mw 6 occurred in north-eastern Iran. It was not possible to relate a fault to the earthquake, according to the reports of the Iranian seismological center (IRSC) and the International Institute of earthquake engineering and seismology (IIEES) of Iran. The association of the earthquake to the western part of the Fariman fault or to the southern end of the Kashafroud fault is not possible. In this study, data from the stations of the aforementioned agencies was used to model the earthquake waveforms, and an effort was made to find the focal mechanism of this earthquake, investigate it, and also to eliminate the ambiguities that exist in determining the fault plane of the earthquakes using the Hypocenter-Centroid (H-C) method, due to the higher accuracy in simulating the waveforms and finding the centroid point of earthquakes in local and regional distances. We obtain the fault plane with a strike of 324 and dip of 44 degrees, which indicates the northwest-southeast trend, parallel to the trend of the Kashafroud fault. This has good agreement with the results of other resear-chers.

Keywords:
H-C Method; Focal Mechanism; Kashafroud fault; ISOLA

1. Introduction

On April 5, 2017, an earthquake occurred in Iran with a magnitude of Mw 6.0, about 30 km from the Sefidsang region and 80 km from Mashhad city in Razavi Khorasan province. The Sefidsang event occurred in an area where its direct association with a known fault was not possible. It was not possible to attribute this event to the activity of the western part of the Fariman fault or the southern end of the Kashafroud fault, so much research has been conducted to find the fault plane and geologic fault that caused this event. In this research, a study is performed to distinguish the fault plane from the auxiliary plane using the H-C method in ISOLA software (Zahradnik & Sokos, 2019). A large number of faults and the occurrence of frequent earthquakes during the past decades highlight the need for a better estimation of the seismic potential in the region. Earthquake focal mechanisms are important for studying the tectonic seismicity of an area and understanding the physical processes applied to a fault during an event and in stress analysis, therefore determining the main slip plane mainly through field observations, such as determining the exact location of aftershocks or by using common methods in seismology is necessary. In some studies, the pattern of slip propagation (the amount of slip at each point of the fault plane) is determined for both fault planes, and the plane that best fits the data is known as the main fault plane. The use of such methods is relatively time-consuming and expensive, and in many cases, the required information is not available. That includes suitable methods for detecting the fault plane of large earthquakes that do not have surface outcrops or the possibility of using geological evidence to detect the plane. One of the methods to minimize the cost is the H-C method. In this method, the estimation of the fault plane is almost fast.

2. Seismotectonics

The plateau of Iran is characterized by features such as active faulting, young volcanic activity, and high altitudes among the Alpine-Himalaya Mountain belt. Geological, seismological and geophysical evidence show that the land of Iran has a high earthquake potential and people's lives and property are always under the threat of this natural phenomenon. The tectonic changes that have occurred in Iran have been associated with crustal shortening and faulting, which is the result of its convergence and pressure. It is located between the Arabian and Eurasian plates (Mirzaee et al., 1998). In the meantime, north-eastern Iran, which is in the Koppeh Dagh seismic province, is an in-plate environment, where in the eastern and central areas of Koppeh Dagh, there is a system of faults with a right-handed component with an east-southeast and west-northwest trend (Qochan-Bojnord area). In the western areas, there is a fault system with a left-handed component with a northeast-southwest trend. Among the most important faults in this region, we can mention the Koppeh Dagh fault zone, Freeman fault, Kashafroud fault, Torbat Jam fault and Binaloud fault (Tchalenko et al., 1975).

Kashafroud fault is a part of the important structure of Atrak-Kashafroud valley. Atrak Valley-Kashafroud is the place of the on-land suture between Koppeh Dagh (Eurasia) and Eastern Alborz-Binaloud (Central Iran) (Motaghi et al., 2012). The length of this fault reaches 120 km (Hesami Azar, 2007) and has a compressive mechanism.

Aghar Fariman fault has two segments. Both Aghar and Fariman segments are 80 km long and constitute a fault with an approximate length of 120 km with a generally northwest-southeast direction. The fault passes from the southeast of Fariman City. These fault fragments with the reverse mechanism and slope towards the southwest caused the Cretaceous ophiolitic mixtures (from the southwest) to be pushed onto the Eocene conglomerate (to the northeast). In addition, the Quaternary Pliocene deposits cut along the Freeman fault indicate its young age. It is worth mentioning that despite the fact that accurate dating or seismic data has not been reported for these two fault segments, according to the geological evidence, Hesami Azar (2007) introduced them as powerful faults. Among the new researches in the area, we mention Khosravi et al. (2019) that by determining upper crustal structure of Fariman region, concluded the existence of a new fault patch in the area in continuation of the Mozduran fault.

Figure (1) shows the seismotectonic map of the studied area along with the focal mechanism of this earthquake from different seismographic centres around the world.

The detailed local map of the region is illustrated in Figure (2).

3. Method

In this research, ISOLA software was used to investigate April 5, 2017, Sefidsang Khorasan earthquake with a magnitude of 6.1, and the full waveform inversion is employed. The data from the stations of the IRSC, Institute of Geophysics, University of Tehran, and IIEES are used to model the waveforms and determine centroid moment tensor (CMT). Since 2006, the use of ISOLA to determine CMT of seismic events has become common. This method was devised and developed by Zahradnik and Sokos (2019) using the complete calculation of Green's functions with the discrete wavenumber method (Bouchon, 1981) for local and regional distances. One of the advantages of

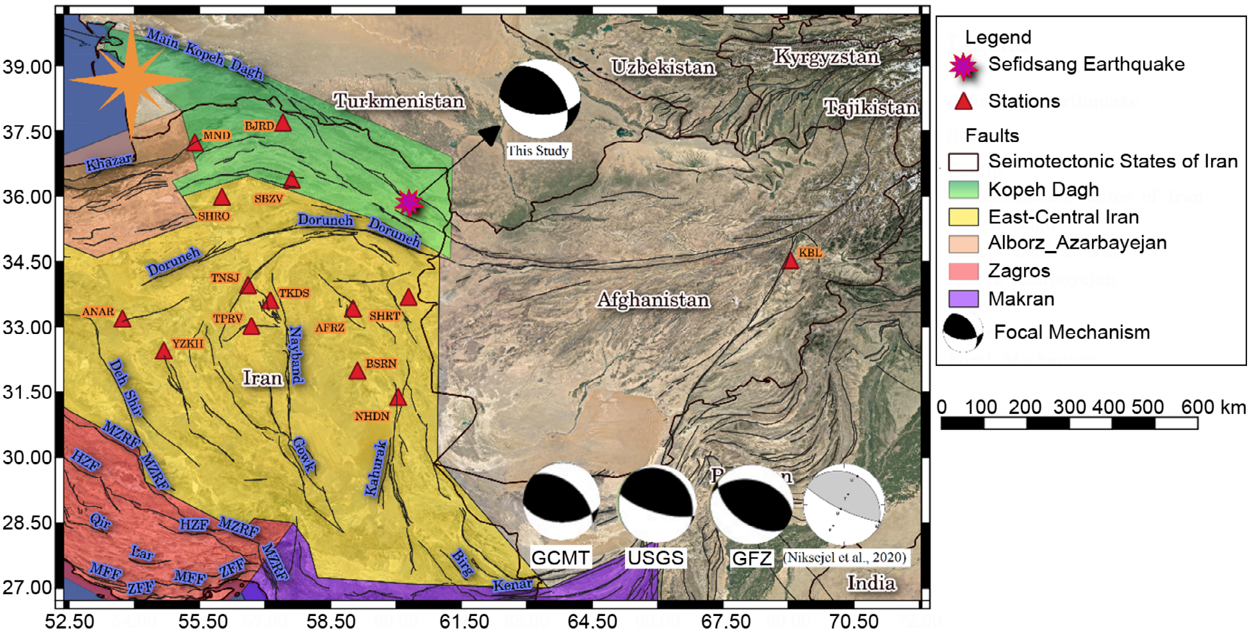

Figure 1. Seismotectonic and station map of the studied area along with the focal mechanism of the earthquake from different seismological centres around the world. One reported focal mechanism is from Niksejel et al. (2021) paper shown in different colours. The epicentre location is from IRSC. Details of northeastern seismotectonic provinces are from Mirzaee et al. (1998), and the fault lines are extracted from Hesami Azar et al. (2003).

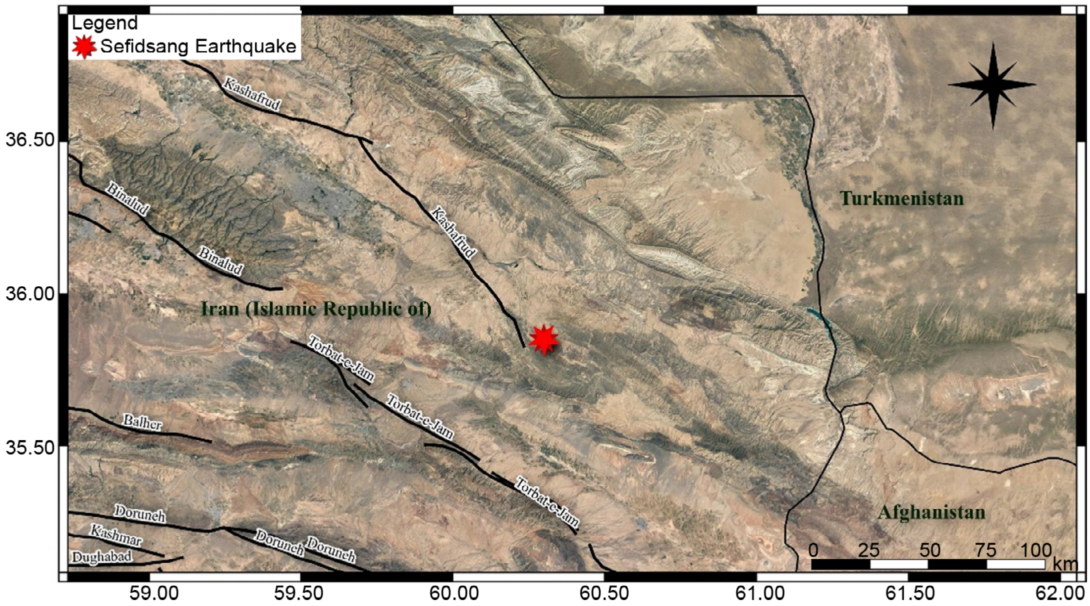

Figure 2. Detailed seismotectonic map of the studied area. The seismotectonic provinces are shown in the map on bottom-right corner (Mirzaee et al., 1998). The faults are drawn according to Hesami Azar et al. (2003).

this method is that due to the use of local and regional data, higher frequencies can be modelled, and it is possible to achieve higher accuracy in obtaining fault parameters. The H-C method was introduced by Zahradnik et al. (2009) to determine the fault plane and was used for an earthquake in Greece with a magnitude of 6.3.

In the ISOLA method, the complete waveforms of the local or regional data are used to obtain the moment tensor. This procedure takes place in the time domain. First, instrumental correction is applied to the seismograms. Then, a frequency band is employed to filter the observed data, and the velocity seismograms are converted to displacement. Then, by calculating Green's functions, synthetic seismograms at different stations are calculated. Linear inversion by ordinary least squares is performed in the time domain. The synthetic seismograms are then compared to observed seismograms.

ISOLA determines CMT solution. The CMT solution includes the simultaneous solution of the spatial and temporal dependence of the point source with its six independent components of the moment tensor. Therefore, by leaving aside the volumetric part of the moment tensor, it is possible to determine the contributed percentage of the remaining moment tensor into the best double-couple (DC) and compensated linear vector dipole (CLVD) parts.

The H-C method is applicable in conditions where the solution of the moment tensor has a high percentage of DC, because, in such a situation, it is possible to assume that the fault nodal planes are flat. Otherwise, the source of the earthquake should be considered as a superposition of two or more events or the tensor of two DC sources.

In solving the mechanism of the earthquake source, two nodal planes are determined. Proving which plane is really the main plane (fault) and which is the auxiliary plane is very important for seismologists (Zahradnik et al., 2009). The importance of this issue lies in its application to perform seismotectonic studies. Earthquakes with medium depth (such as Makran earthquakes) rarely have known fault planes, because the rupture of these earthquakes rarely extends to the surface of the earth, and they also mostly lack aftershocks. However, the knowledge of these planes helps a lot to understand the geodynamic model of the subducting zone and the stress field on a regional scale, that is, one of the most important advantages of knowing the main plane among the two nodal planes is the important role it can play in stress analysis.

The other advantage is identifying active hidden faults, a knowledge that can greatly contribute to a better understanding of earthquake risk analysis. Under certain conditions, a fault can be well-mapped with the spatial distribution of a large number of aftershocks. Of course, this technique has many limitations. One of these limitations is the inability to accurately determine the location of weak aftershocks in the absence of dense networks. In addition, some of these earthquakes do not have aftershocks on the main earthquake fault plane (this condition is observed in moderate-depth earthquakes).

The importance of knowing the fault plane does not end here. In cases where the earthquake is located geologically near to or on a known fault, this method can still be considered an independent benchmark because the known faults may also have complex tectonics at greater depths.

The most important advantage of the method used is the quick identification of the fault plane. If this work can be done almost online, it can play a vital role in simulating the strong motion of the earth (motion map). Here, the rapid identification means hours after the earthquake.

The H-C method is a simple and new method that can be implemented quickly if the centroid from CMT and the epicenter are available. In the methods of determining the location of an earthquake, based on the time of the seismic phases, the location of the beginning of the rupture, or the epicenter of the earthquake is determined. Therefore, this location is considered as the starting point of the rupture (H). However, the CMT solution obtained from the modeling of long-period waves approximates the location of spatial averages of the earthquake's distribution of seismic moment (C). In addition, by determining the moment tensor elements in the CMT solution for the case of double-couple source, the values of the strike, dip, and slip angles of the two main and auxiliary planes that pass-through C can be determined.

In this research, to calculate Green's functions and to improve the results, the velocity models of both IRSC and IIEES were used. IRSC model was selected as the most compatible model with the region for final processing (Table 1). Examining local and regional data allows us to obtain more details during modelling. We tried to determine the geometry of the fault planes and centroid (C). Due to the nonlinearity of this part of the problem, the centroid location is determined by grid search. At first, we search for optimum source location among potential sources on a vertical profile under epicentre. The search for depth was performed from three to 17 km with a step of 1 km. The optimum depth was determined at six km. Figure (3) shows the graph of correlation versus depth which shows the optimum depth of six km with a favourable resolution.

After finding the depth, the eastward and northward shift of the centroid is determined by constructing a horizontal grid plane at the optimum depth. In this stage, we used 25 sources with 2 km distance in between and the number of 5 sources along the NS and 5 sources along the EW orientation.

Table 1. IRSC velocity model used in this research.

Depth (km)	Vp (km/sec)	Vs (km/sec)	Density (g/cm^3)
0	5.38	3.057	2.776
7	5.95	3.381	2.89
12	6.15	3.494	2.93
20	6.42	3.648	2.984
47	8.06	4.58	3.312

In the inversion steps, the frequency range of 0.02-0.05 Hz was used. The best frequency range is selected based on the best value of the variance reduction (the largest value close to one) for the individual components of the stations. In this way, the inversion has been done many times for the event by choosing different frequency ranges and the best solution has been considered.

H-C method essentially works by finding the location of the centroid. When the two nodal planes were determined, the middle of their inter section constitute the centroid. Furthermore, the location of the hypocenter should also be on one of the nodal planes or near to it due to errors in location and focal mechanism determination. This nodal plane is then suggested as the causative fault of the earthquake under study.

4. Results and Discussions

So far, Khorrami et al. (2022) has been studied the earthquake and identified the Kashafroud fault as the causative fault. In this study, an attempt is made to identify the fault that caused this earthquake by using ISOLA software and its H-C geometric method, modelling regional data waveforms by the position of the hypocentre (H) and centroid (C) of the fault plane.

The focal mechanism obtained in this study for this earthquake is a reverse type with a dextral strike-slip component, which is in good agreement

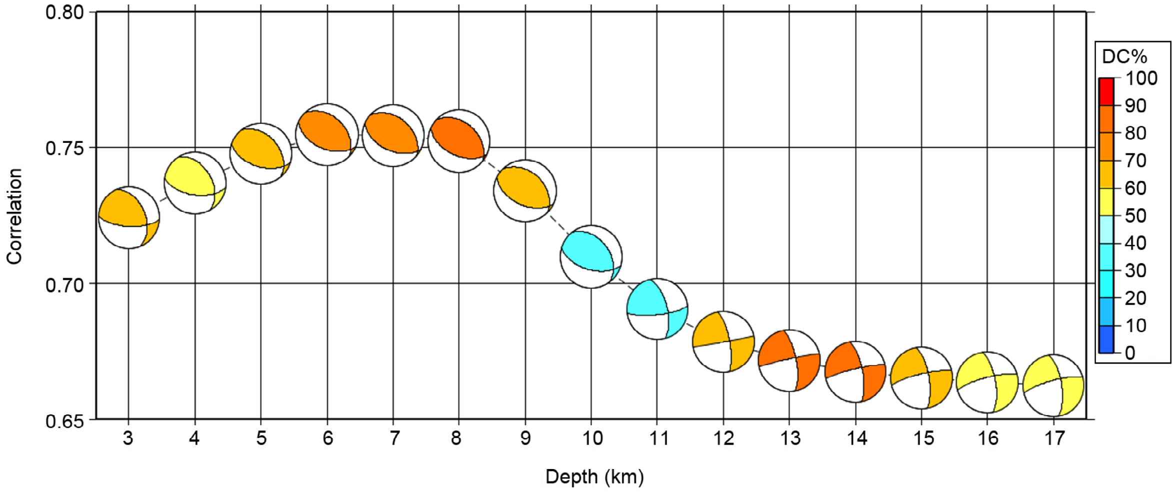

Figure 3. The plot of correlation of observed and synthetic seismograms versus depth. The optimum depth is determined to be at six km.

with the mechanism obtained from the global CMT project. Figure (4) shows the matching of the observed and synthetic waveforms. As it is clear in the figure, the observed and synthetic mappings are in good agreement for most of the components of the stations. Since a few waveforms did not show a good agreement, they were removed in the inversion process.

Different locations of hypocentres including the obtained relocation of IRSC were used and tested in this study and the best location that leads to the optimum result was selected. By using the H-C method and with the three-dimensional drawing of the nodal planes obtained and according to the placement of points H and C, it is determined that a plane with a Strike of 324 degrees and a Dip of 44 degrees is the fault plane.

In Figure (5), the final output of the CMT solution for the earthquake is presented. In the figure, the earthquake mechanism, the percentage of the double couple of the moment tensor, and also the value of the variance regression is shown. The mechanism is drawn as a beachball after finding the coordinates of the centroid. As it is clear from the figure, the obtained focal mechanism has an approximate northwest-southeast trend. In the results, the value of the condition number, which is specified by the minimum and maximum

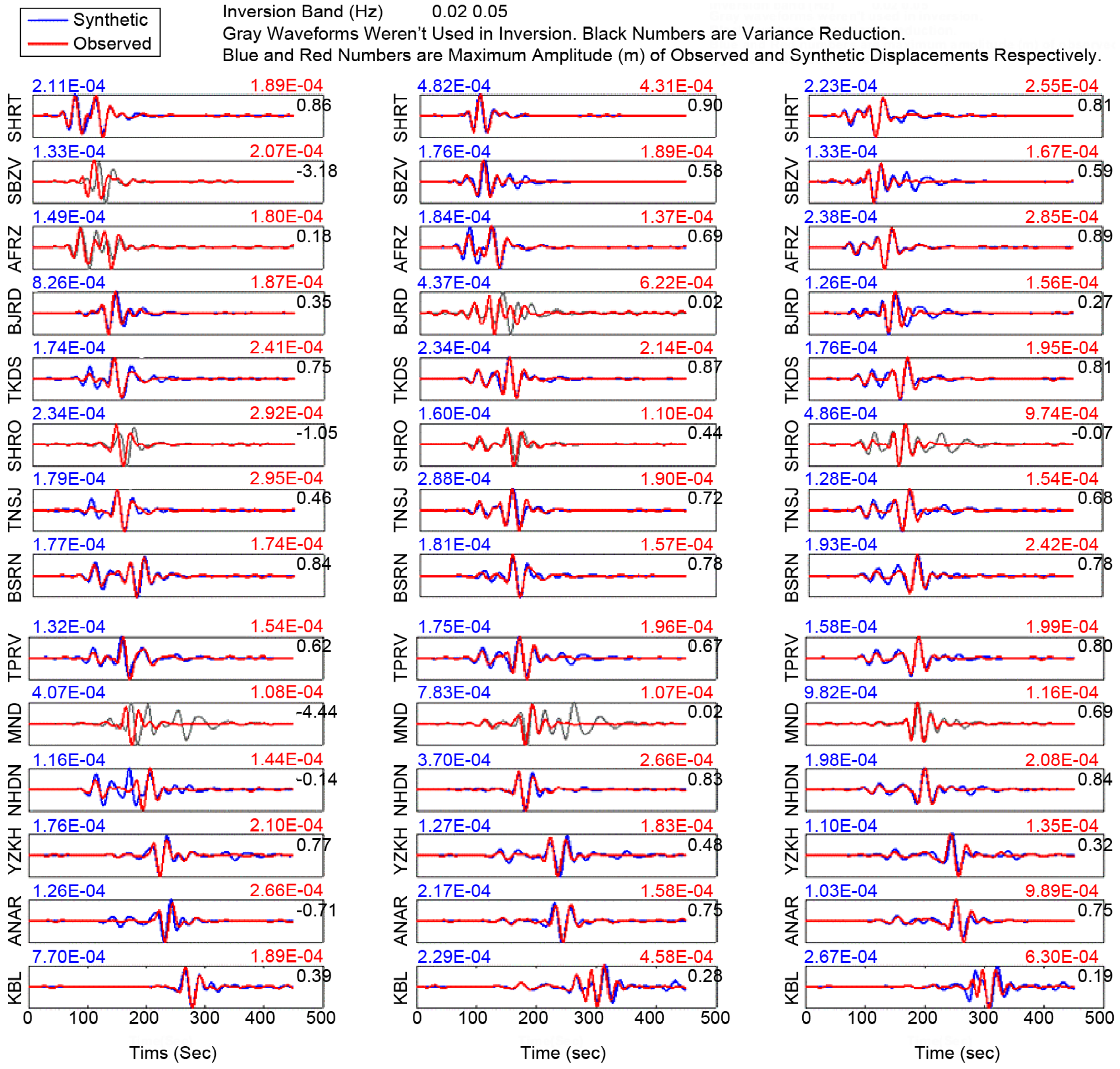

Figure 4. Comparison of the observed waveforms at the stations and the generated synthetic waveforms for the earthquake that occurred on April 5, 2017, at 2:32. The black number above the component of each station represents the variance reduction and the blue numbers are the maximum observed displacement in meters. The components shown in gray are removed in the inversion process.

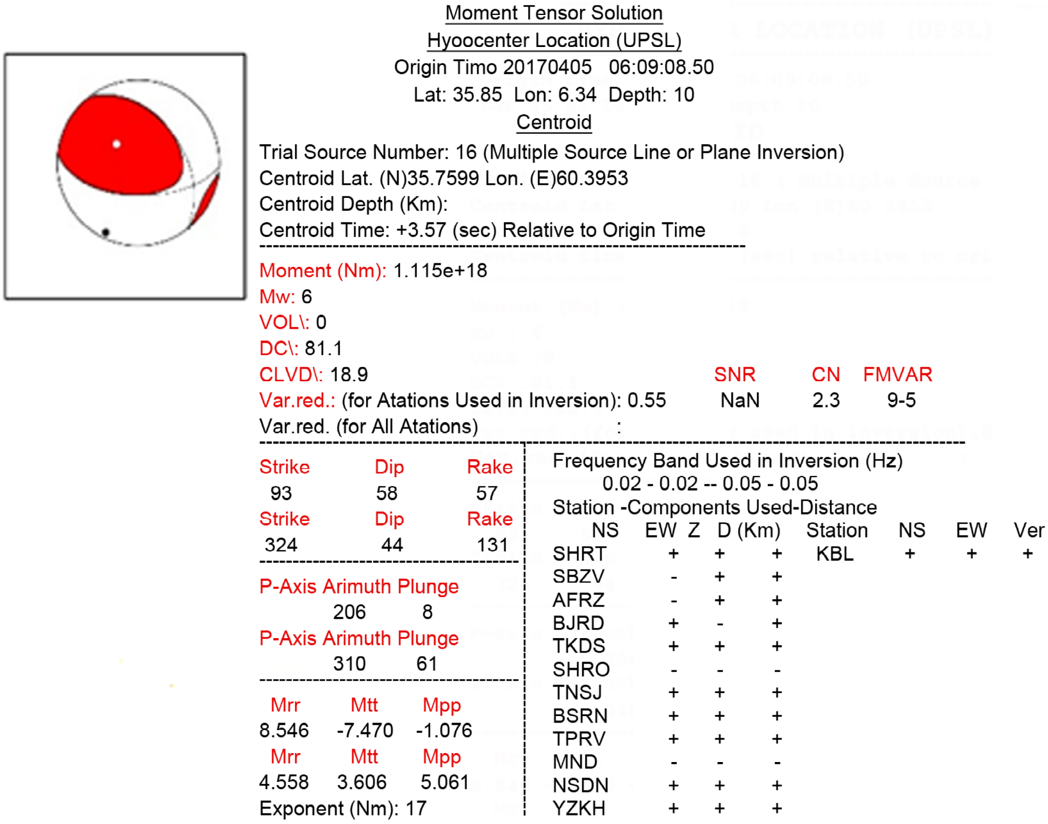

```
                         Moment Tensor Solution
                       Hyoocenter Location (UPSL)
                    Origin Timo 20170405   06:09:08.50
                      Lat: 35.85  Lon: 6.34  Depth: 10
                                Centroid
Trial Source Number: 16 (Multiple Source Line or Plane Inversion)
Centroid Lat. (N)35.7599 Lon. (E)60.3953
Centroid Depth (Km):
Centroid Time: +3.57 (sec) Relative to Origin Time
--------------------------------------------------------------
Moment (Nm): 1.115e+18
Mw: 6
VOL\: 0
DC\: 81.1
CLVD\: 18.9                                       SNR      CN    FMVAR
Var.red.: (for Atations Used in Inversion): 0.55   NaN      2.3     9-5
Var.red. (for All Atations)                :
--------------------------------------------------------------------------------
Strike        Dip         Rake  | Frequency Band Used in Inversion (Hz)
 93           58           57   |       0.02 - 0.02 -- 0.05 - 0.05
Strike        Dip         Rake  | Station -Components Used-Distance
324            44          131  |        NS    EW  Z  D (Km)  Station   NS    EW    Ver
--------------------------------| SHRT          +     +      +    KBL     +     +     +
P-Axis Arimuth Plunge           | SBZV          -     +      +
         206        8           | AFRZ          -     +      +
P-Axis Arimuth Plunge           | BJRD          +     -      +
         310        61          | TKDS          +     +      +
--------------------------------| SHRO          -     -      -
  Mrr       Mtt       Mpp       | TNSJ          +     +      +
8.546     -7.470    -1.076      | BSRN          +     +      +
  Mrr       Mtt       Mpp       | TPRV          +     +      +
4.558     3.606      5.061      | MND           -     -      -
Exponent (Nm): 17               | NSDN          +     +      +
                                | YZKH          +     +      +
```

Figure 5. Final output of the CMT solution for the earthquake occurred on April 5, 2017, calculated in this study. The centroid section in the figure shows the optimal latitude, longitude, and depth obtained for the centroid. The third part shows the magnitude of the optimized moment tensor and the amount of seismic moment in Newton meters. The next part shows the amount of variance reduction obtained by incorporating all stations in the inversion operation. It also shows the percentage of a double couple of the moment tensor. In the fourth part, the angles of strike, dip, and rake obtained to solve the centroid mechanism are inserted; finally, it shows the CMT mechanism and the map of the earthquake location and the stations used in this research. The figure contains the obtained values of condition number and also FMVAR measure for uncertainty.

eigenvalues of the system matrix (G-1G) is shown. The condition number measures the multicollinearity of this matrix which contains the data kernel G in a linear system of algebraic equations of d = Gm, where d is the vector of observed data and m is the six independent components of the moment tensor. G has six columns for each elementary seismogram of elementary focal mechanisms, which are calculated from displacement records of Green's functions. The lower the condition number is, the better as it shows that the obtained answers are more reliable. This number is a relative value, but in most cases, an amount lower than 10 is usually suitable. As a measure of uncertainty, FMVAR is determined to be between 5-9 degrees for different stations. It is defined as the mean Kagan angle (Kagan, 1991) of all acceptable solutions in terms of the best-fit solution.

Figure (6) shows a three-dimensional plot of the nodal planes, showing the plane with Strike 324 and dip 44 degrees (red plane) as the fault plane (Strike almost to the north) from five different views.

Khorrami et al. (2022) investigated the aftershocks of the Sefidsang earthquake for the determination of the fault that caused this earthquake using cross-correlation of waveforms and catalog data. The relocated hypocenters of the aftershocks indicate the concentration of earthquakes in an almost circular way that does not show any particular trend. In order to better observe the depth trend, they use two transverse sections. One section is perpendicular to the trend of the northwest-southeast structures of the earth (perpendicular to the possible continuation of the Kashafroud fault) and the other is along the trends of the observed topography. According to the form of the collection of aftershocks, no specific trend can be found. The cross-section of the data given on

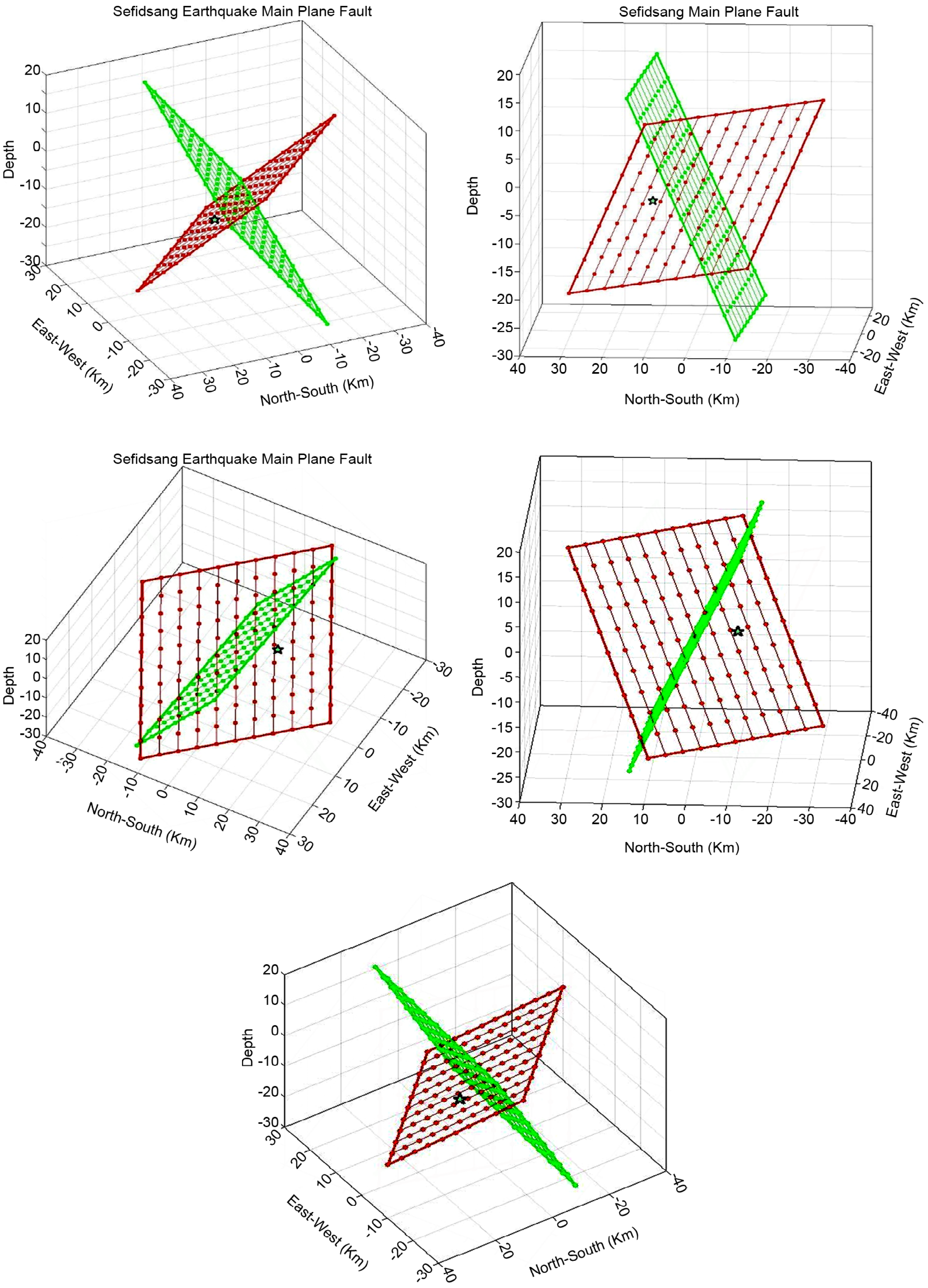

Figure 6. Three-dimensional plot of the nodal planes from five different views, showing the plane with Strike 324 and dip 44 degrees (red plane) as the fault plane (Strike almost to the north). The start shows the hypocenter and the centroid is in the middle of the intersection of the two nodal planes. The distance of the centroid to the hypocenter of the earthquake is estimated to be 11.18 km and the distance of hypocenter with the closest plane is 1.28 km, which shows the errors in determining hypocenter and focal planes.

Table 2. The specifications of the Sefidsang earthquake along with its focal mechanisms determined by different agencies.

No	Lat. (N)	Long. €	Depth (km)	Mag (ML)	Strike1 Dip1 Rake1	Strike2 Dip2 Rake2	Foc. Mech.	Agency
1	35.776	60.436	11.5	6.1	105 73 80	316 20 120		USGS
2	35.81	60.37	12	6.0	91 44 59	312 53 117		GCMT
3	35.74	60.46	15	6.1	125 52 103	285 39 73		GFZ
4	35.7599	60.3953	10	6.0	93 58 57	324 44 131		This Study

the first profile shows the trend of the aftershocks with a slope of about 45 degrees towards the northeast.

Table (2) compares the obtained focal mechanism in this study and those of other agencies. Other than agencies, Niksejel et al. (2021) also determined the focal angles of Sefidsang earthquake with its beachball shown in Figure (1).

5. Conclusion

According to the results of the H-C method, it can be observed that, although in this earthquake, the distance between the hypocentre and the centroid was 11.18 km; it can be acknowledged that the main plane of the causative fault has a strike of 324 degrees and a dip of 44 degrees. This clearly confirms the results of other researchers who worked on the causative fault of the earthquake, such as Khorrami et al. (2022) and Ghayournajarkar and Fukushima (2020).

In their research, Khorrami et al. (2022), by examining the depth sections on two profiles, one in the northwest-southeast direction and the other in the direction perpendicular to the first profile; determined that the slope of the fault plane is about 45 degrees toward the northeast and accordingly, the direction of the fault is northwest-southeast. They showed that the earthquake is associated with the Kashafroud fault. In addition, according to Ghayournajarkar and Fukushima (2020), the dip of the northeast fault model is more consistent, and their desired fault model has a Dip of 47.4 degrees. Furthermore, Nedaei and Alizadeh (2021) in a study on Coulomb stress change pattern and aftershock distribution showed that the Coulomb stress field by regional stress is compatible with both nodal planes while aftershock distribution affirms the nodal plane with 316 degrees strike and 20 degrees dip to the north as the fault; which is consistent with the results of this study.

Acknowledgments

We are very much thankful to the International Institute of Earthquake Engineering and Seismology (IIEES) and Iranian Seismological Centre (IRSC), Institute of Geophysics, University of Tehran for providing the waveforms for this study.

References

Bouchon, M. (1981). A simple method to calculation green's function for elastic layered media. *Bulletin of the Seismological Society of America*, *71*, 959-971.

Ghayournajarkar, N., & Fukushima, Y. (2020). Determination of the dipping direction of a blind reverse fault from InSAR: case study on the 2017 Sefid Sang earthquake, north-eastern Iran. *Journal of the Earth and Space Physics*, *72*(1), 1-15.

Hesami Azar, Kh. (2007). *Seismotectonics Section of the Report of Earthquake Risk Estimation Studies and Geotechnical Earthquakes in the Construction of Imam Reza Holy Shrine*. International Institute of Earthquake Engineering and Seismology, Tehran, Iran.

Hesami Azar, Kh., Jamali, F., Tabassi, H. (2003). *Major Active Faults of Iran (Map)*. Ministry of Science, Research and Technology, International Institute of Earthquake Engineering and Seismology (IIEES).

Kagan, Y.Y. (1991). 3-D rotation of double-couple earthquake sources. *Geophysical Journal International*, *106*(3), 709-716.

Khorrami, Z., Moradi, A., & Songhori, A. (2022). The relocation of April 5th, 2017 Sefid-Sang Earthquake aftershocks sequence using waveform cross-correlation and double-difference techniques. *Journal of the Earth and Space Physics*, *3*(48), 541-555.

Khosravi, H., Javan Doloei, G., Safari, M., Shahrokhim, E., (2019). Seismic analysis and determination of upper crustal structure of Fariman region using 3D seismic tomography. *The First National Conference on Signal and Image Processing in Geophysics,* Shahrood University of Technology.

Mirzaei, N., Gao, M., & Chen, Y.T. (1998). Seismic source regionalization for seismic zoning of Iran: Major seismotectonic provinces. *Journal of Earthquake Prediction Research*, *7*, 465-495.

Motaghi, K., Tatar, M., & Priestley, K. (2012). Crustal thickness variation across the northeast Iran continental collision zone from teleseismic converted waves. *Journal of Seismology*, *16*, 253-260.

Nedaei, M., & Alizadeh, H. (2021). New insights into the 2017 Sefidsang earthquake by Coulomb stress change pattern and aftershock distributions: implication for active tectonics of NE Iran. *Geopersia*, *11*(1), 23-42.

Niksejel, A., Shomali, Z.H., Cesca, S., & Moradi, A. (2021). Towards a regional, automated full moment tensor inversion for medium to large magnitude events in the Iranian plateau. *Journal of Seismology*, *25*, 653-669.

Tchalenko, J.S. (1975). Seismicity and structure of the Kopet Dagh (Iran, USSR). *Philosophical Transactions of the Royal Society*, London, Ser. A, 278, 1-28

Zahradnik, J., & Sokos, E. (2018). ISOLA Code for Multiple-Point Source Modeling-Review. In: D'Amico, S. (eds) Moment Tensor Solutions. *Springer Natural Hazards*. Springer, Cham. https://doi.org/10.1007/978-3-319-77359-9_1.

Zahradnik, J., & Sokos, E.N. (2019). 'ISOLA Code for Multiple-Point Source Modeling - Review'. In: D'Amico, S. (Ed.), *Moment Tensor Solutions: A Useful Tool for Seismotectonics*. Springer.

Zahradnik, J., Sokos, E., & Tselentis, A. (2009). *Quick Identification of the Fault Plane for Mw 6.3, Earthquake South of Crete, Greece July 1, 2009*. Report to EMSC issued on July 1st.